

From Retrodiction to Bayesian Quantum Imaging

Fiona C. Speirits, Matthias Sonnleitner, Stephen M. Barnett

INTRODUCTION

We employ quantum retrodiction to develop a robust Bayesian algorithm for reconstructing the intensity values of an image from sparse photocount data, while also accounting for detector noise in the form of dark counts. This method yields not only a reconstructed image but also provides the full probability distribution function for the intensity at each pixel. We use simulated as well as real data to illustrate both the applications of the algorithm and the analysis options that are only available when the full probability distribution functions are known. These include calculating Bayesian credible regions for each pixel intensity, allowing an objective assessment of the reliability of the reconstructed image intensity values.

STATE PREPARATION AND RETRODICTIVE PROBABILITIES

It is common to consider state preparation in a *predictive* manner: Alice prepares a state, sends it to Bob and predicts what he will receive. Image reconstruction, however, can be better addressed in a *retrodictive* manner: if Bob received a state, what can he say about what Alice sent? For two events in time, a and b , the predictive and retrodictive probabilities can be written as:

$$p(\bar{a}|b) \quad \text{RETRODICTIVE}$$

These probabilities are inherently related through Bayes' Rule:

$$p(a|b) = \frac{p(b|a)p(a)}{p(b)}$$

In the context of state preparation with Alice and Bob, this corresponds to:

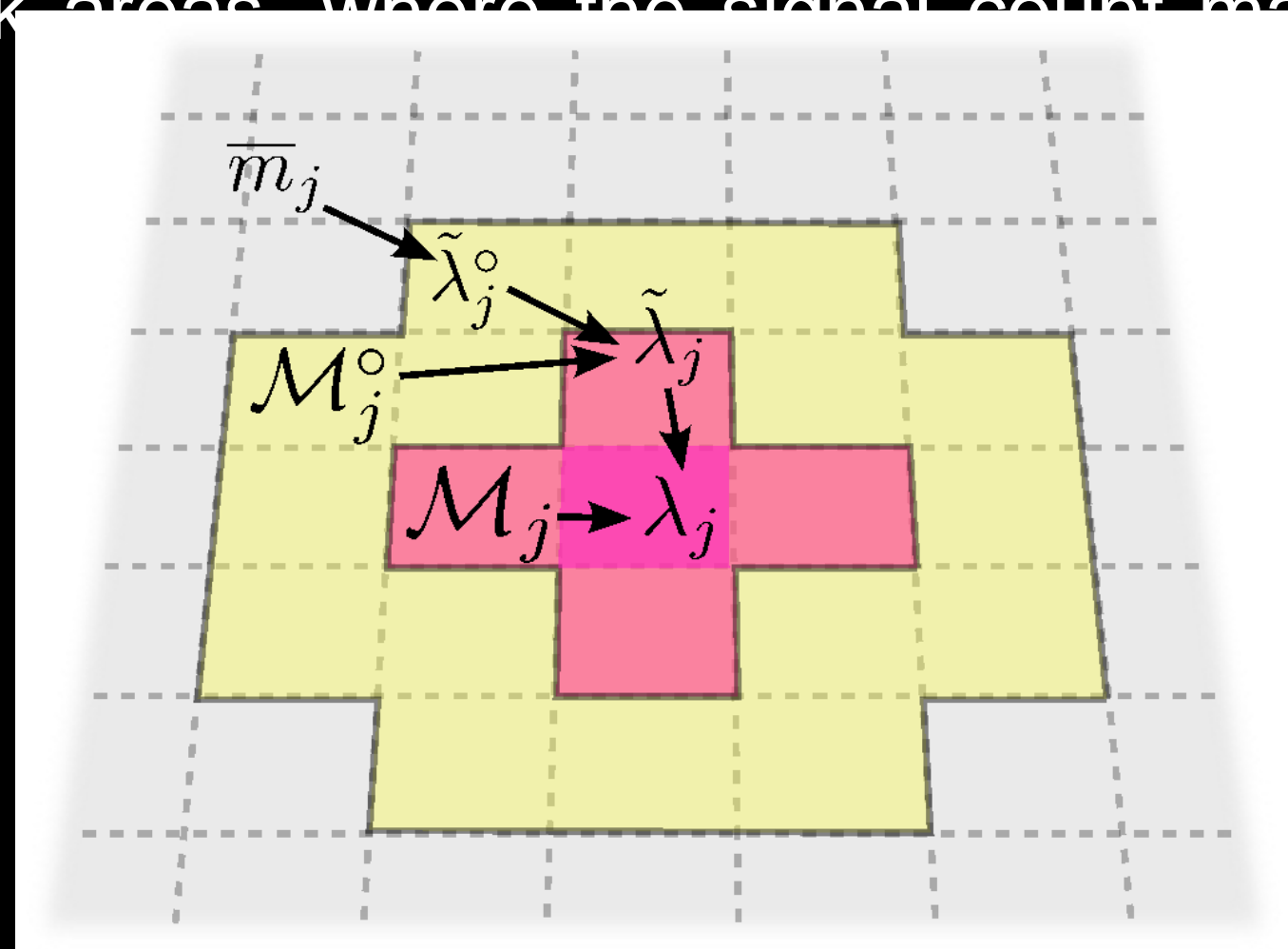
$$p(\text{Alice}) = \frac{p(\text{Alice, Bob})p(\text{Bob})}{p(\text{Bob})}$$

IMAGE RETRODICTION

In image reconstruction, we want to retrodict the original intensity λ , given photocount data from a detector of efficiency η and a dark count rate ϵ (assumed to be uniform across all pixels). Employing a Bayesian inference approach allows us to include information from the surrounding pixels in the form of an entropy maximising prior $\tilde{\lambda}$. This results in a probability distribution function for the intensity at each pixel, given a measured number of counts m :

$$p(\lambda|m, \tilde{\lambda}, \epsilon) = \frac{p(m|\lambda, \epsilon)p(\lambda|\tilde{\lambda}, \epsilon)}{p(m|\tilde{\lambda}, \epsilon)}$$

The prior is constructed from the surrounding pixels \mathcal{M}_j° , using the average number of counts in the rest of the image to prevent a negative prior in very dark areas, where the signal count may be lower than the dark counts:



Constructing the full probability distribution function (pdf) at each pixel also gives a measure of the reliability of the retrodicted intensity values; we can define Bayesian credible regions that enclose e.g. 68.3% of the (pdf) for the narrowest range of intensity λ .

[1] M. Sonnleitner, J. Jeffers and S.M. Barnett, *Image retrodiction at low light levels*, *Optica*, 2(11):950-957 (2015)

[2] P.A. Morris et al., *Imaging with a small number of photons*, *Nature Communications*, 6:5913, (2015)

RESULTS

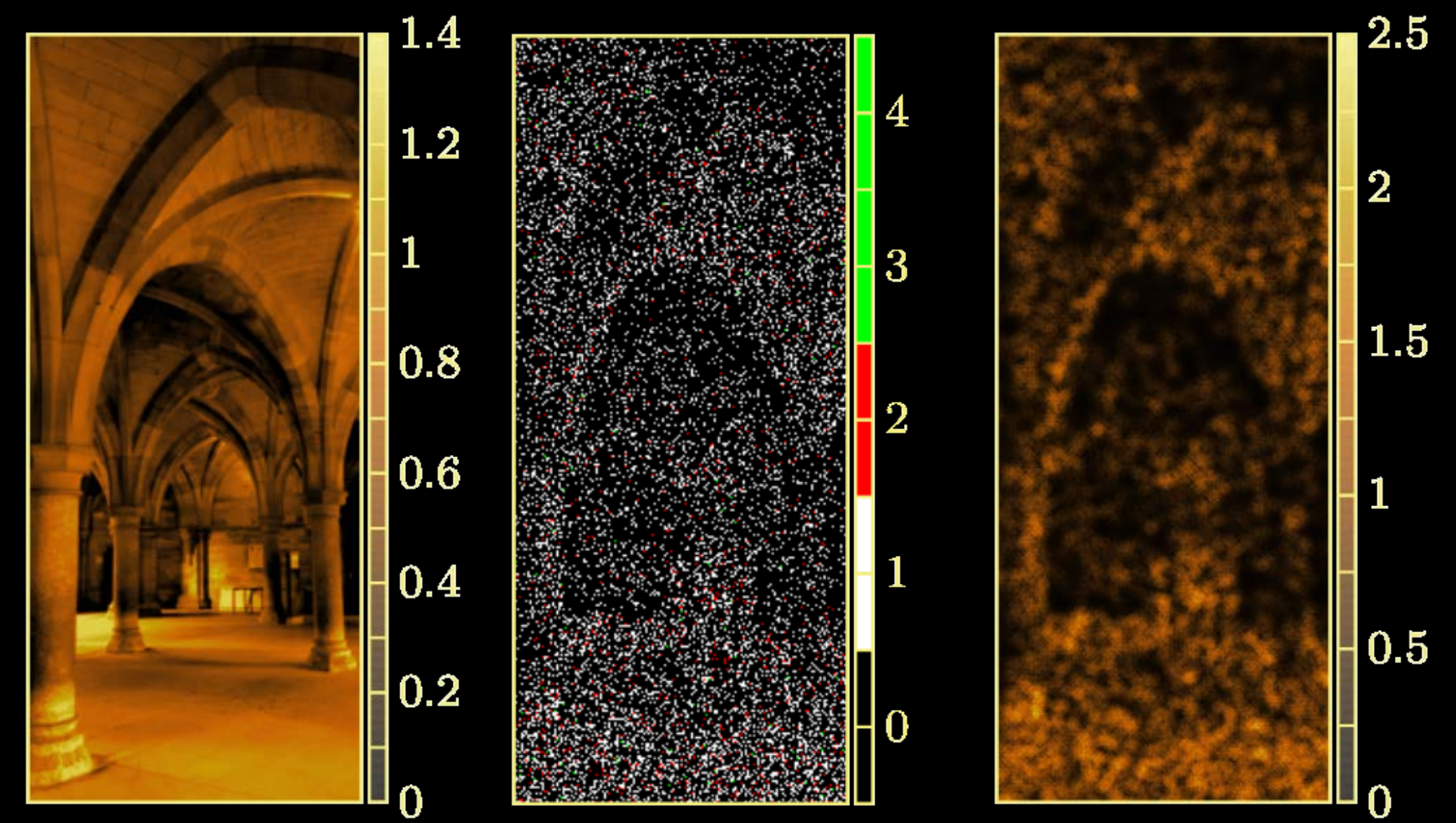


Figure 1: From left to right: the original image; the 'measured' low photocount data, sampled from the original image ($N_p=372 \times 162$ pixels, detection rate $\eta=0.3$, dark-count rate $\epsilon=0.05$, on average $\bar{m}=0.2$ counts per pixel); the reconstructed image produced by the local retrodiction algorithm, obtained by identifying the expectation value of the intensity λ at each pixel.

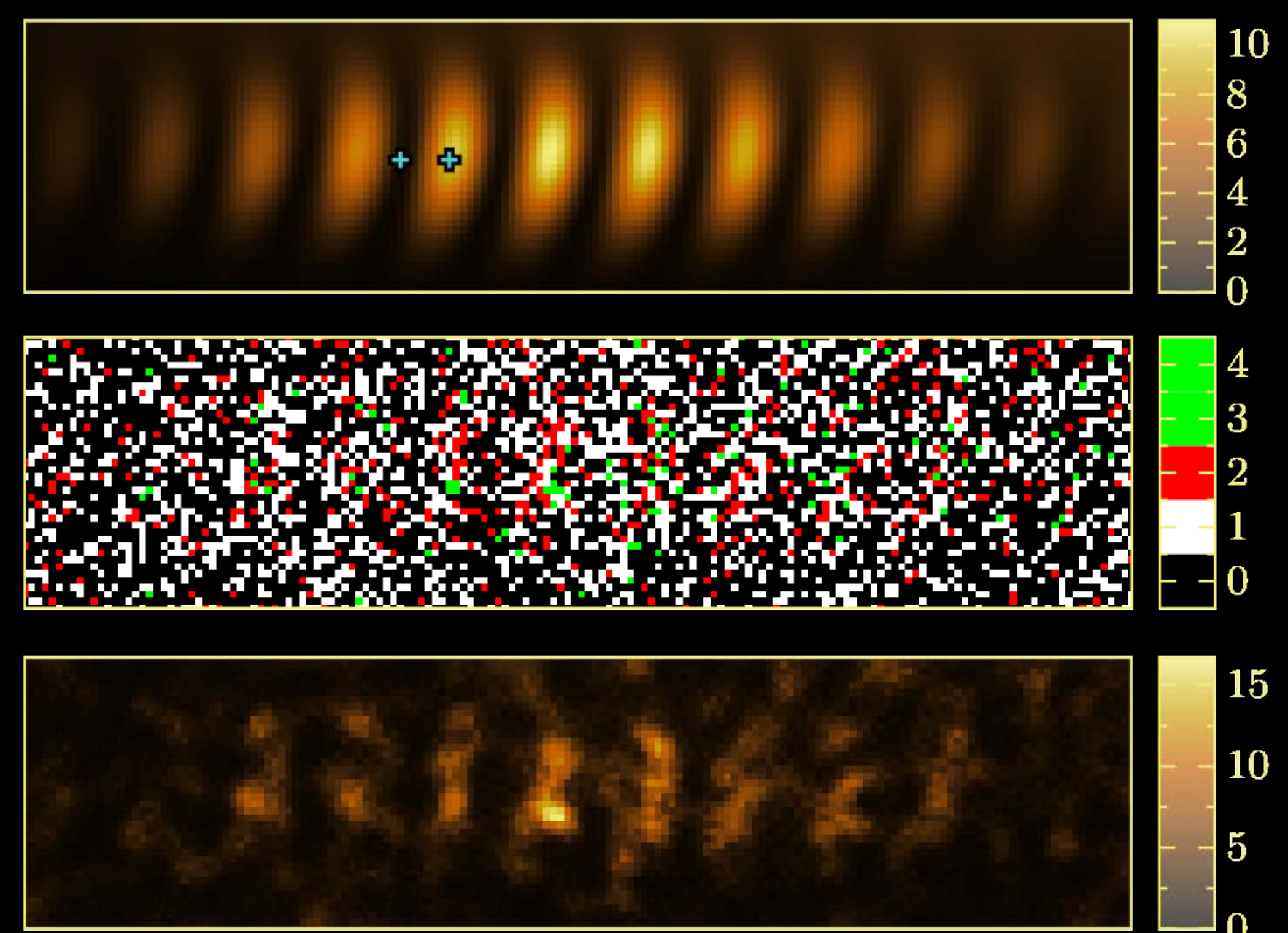


Figure 2: Top: the original image of simulated interference fringes. The crosses are pixels of interest used in Figure 3. Middle: the 'measured' low photocount data, sampled from the original image ($N_p=40 \times 160$, $\eta=0.1$, $\epsilon=0.3$, $\bar{m}=0.5$). Bottom: the retrodicted intensity values, showing the reconstructed image.

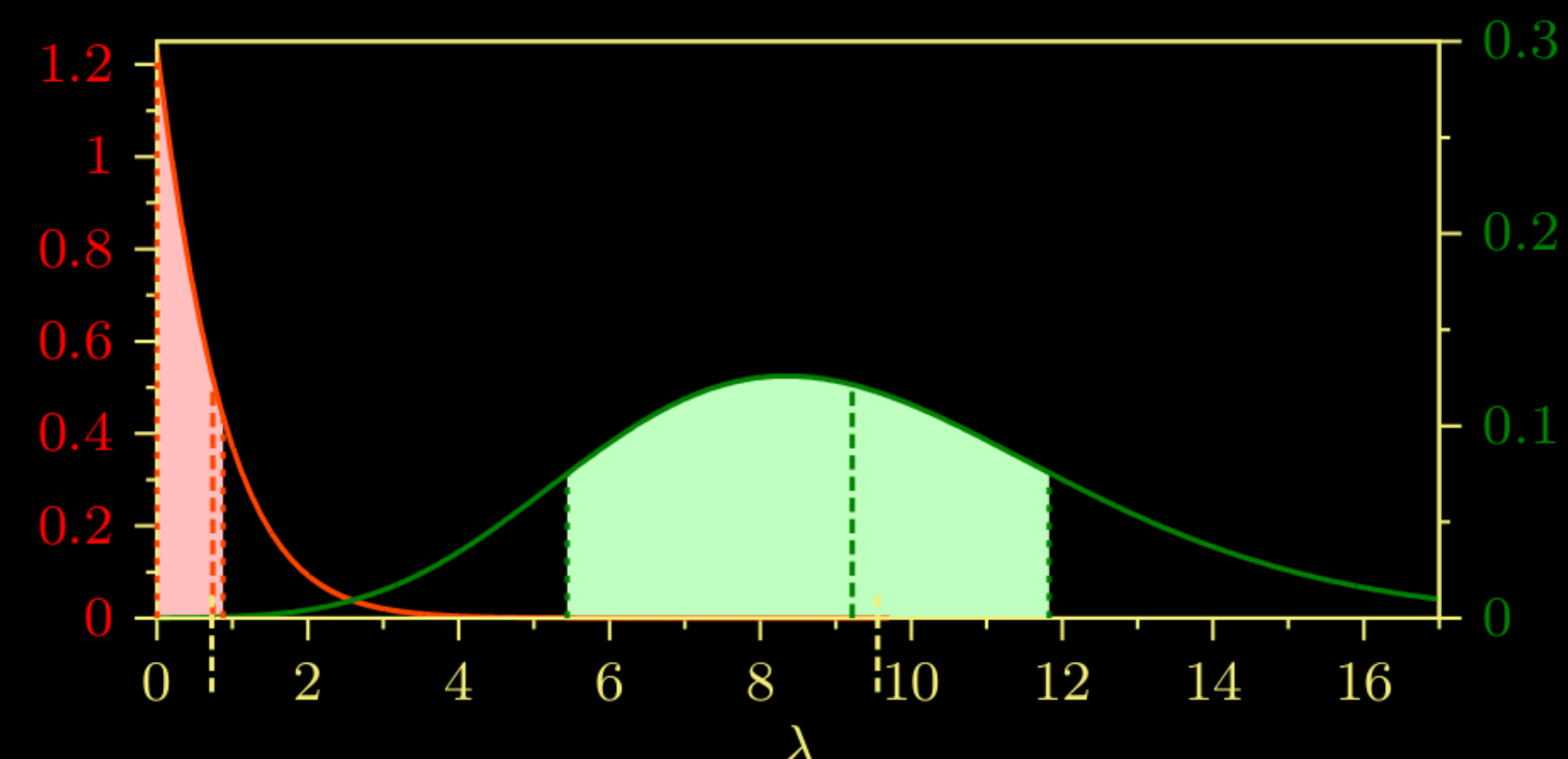


Figure 3: The probability distribution of the reconstructed intensities λ at each pixel of interest, as marked in Figure 2, one dark (red, left vertical axis) and one bright (green, right vertical axis). This allows us to identify the error in λ from the width of the 68.3% credible region (shaded). We also show the expectation value (red or green dotted line) and the 'true' value of the intensity (yellow dotted line below axis), which is only available when using simulated data from a known original image.

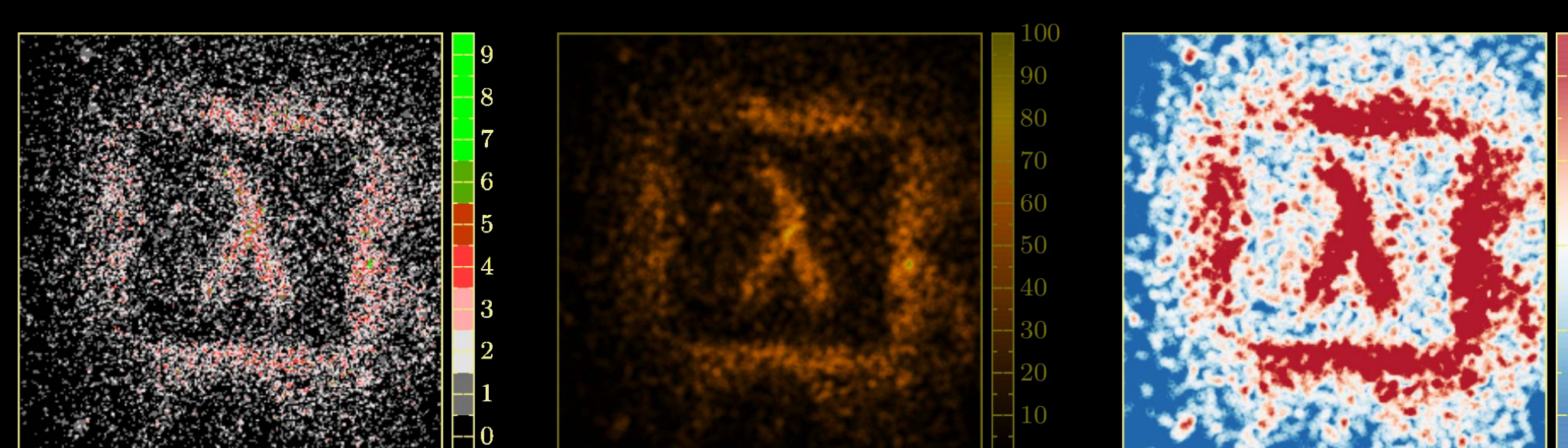


Figure 4: Left: real photocount data from a ghost imaging experiment [2] ($N_p=240 \times 240$, $\eta=0.05$, $\epsilon=0.03$). Middle: the reconstructed image, showing the denoising applications of the retrodiction algorithm. Right: the evidence (in decibels) that the evaluated intensity at each pixel is above the retrodicted image median value.

ACKNOWLEDGEMENTS

The authors would like to thank Reuben Aspden and Miles Padgett for kindly providing us with their experimental ghost imaging data. This work was supported by the EPSRC through the quantum hub QuantIC EP/M01326X/1, the Austrian Science Fund FWF (J 3703-N27) and the Royal Society.